Modeling approach for HexMC discontinuous composite materials based on probabilistic laminate analogy

Paolo Feraboli[1], Marco Ciccu[2]
University of Washington, Seattle, WA

Abstract

Recent composite technology research and development efforts have focused on discontinuous carbon fiber/ epoxy molding systems derived from chopped aerospace-grade unidirectional tape prepreg. Although the average elastic modulus of this material has been shown to be as high as that of the continuous tape quasi-isotropic benchmark, experimental measurement by means of strain gage or extensometer has shown variation as high as 20%. Digital image correlation can be used successfully to obtain a full-field strain measurement, and it shows that a highly non-uniform strain distribution exists on the surface of the specimen, with distinct peaks and valleys. This pattern of alternating regions of high and low strain gradients, and which exhibit a characteristic shape and size, can be described in terms of Random Representative Volume Element (RRVE). The RRVE proposed here exhibits random elastic properties, which are assigned based on stochastic distributions. This approach leads to the analysis method proposed here, which is designed to compensate for the fact that traditional methods cannot capture the experimentally observed variation in modulus within a specimen and among different specimens. The method utilizes a randomization process to generate statistical distributions of fractions and orientations of chips within the RRVE, and then applies Classical Laminated Plate Theory to an equivalent quasi-isotropic tape laminate to calculate its average elastic properties. Validation of this method is shown as it applies to a finite element model that discretizes the structure in multiple RRVEs, whose properties are generated independently of the neighboring ones, and then are solved simultaneously. The approach generates accurate predictions of the strain distribution on the surface of the specimen.

[1]Paolo Feraboli, Ph.D., Corresponding Author, Assistant Professor and Director, *Automobili Lamborghini* Advanced Composite Structures Laboratory, Department of Aeronautics and Astronautics, Box 352400 Guggenheim Hall, University of Washington, Seattle, WA 98195-2400
[2] Marco Ciccu, Graduate Research Assistant, Department of Aeronautics and Astronautics, University of Washington

I. Introduction

Recent composite technology research and development efforts have focused on new out-of-autoclave material forms, and automated processes that can markedly increase production efficiencies. The interest of the aerospace community for short fiber composites dates back to the 1960s and the pioneering work of Halpin, Pagano and Kardos [1-3]. Traditionally these have been referred to as Sheet Molding Compounds (SMC) and typically consist of mats of randomly distributed tows or strands of glass or carbon fiber, and sandwiched between films of thermoset resin. In traditional SMC, discontinuous glass or carbon fiber tows or strands are typically 1.0 in. (25.4 mm) long, and are embedded in polyester or vinyl-ester resins, which are well suited for compression molding of near-net shape parts in high production volumes.

In recent years, airframe manufacturers have been proposing the use of high-performance discontinuous systems that are suitable for compression molding of primary structures. The Boeing 787 Dreamliner for example makes use of AS4/ 8552 HexMC® for the window frames [4,5], as well as other secondary structural elements. These mats are processed by consolidating together, in the form of a roll, sheets of randomly distributed "chips", of 2.0 in. length and 0.33 in. width (50.8 mm x 8.4 mm). These chips are obtained from pristine aerospace-grade unidirectional (UD) carbon fiber/ epoxy prepreg AS4/ 8552. Although the raw material cost associated with these chopped systems is higher than the UD prepreg from which they are derived, their suitability to be molded in complex geometries with lower manufacturing costs and at higher rates can justify their adoption to reduce overall part acquisition costs.

The authors have been performing fundamental research on these materials, and previous experimental results have been reported [6-8]. This class of materials, which sits, perhaps uncomfortably in the eyes of the aerospace engineering community, between traditional SMC and prepreg tape, has shown excellent mechanical properties [5,6], particularly for stiffness-dominated designs, since the average modulus reported can be as high as that of the reference quasi-isotropic continuous tape laminate. Furthermore, while tensile strength is less than half that of the reference quasi-isotropic continuous tape laminate, compressive and shear strengths are much closer to those of the reference tape laminate. If material and process are accurately controlled, the variation observed in the measured strength is also relatively low around 6-8%, and competitive with the 4-6% observed for the tape precursor. Results

also show that the distribution of chips is indeed random, yielding in-plane quasi-isotropic elastic and strength properties. These statements have been verified by testing coupons obtained at 0, 45 and 90° directions.

These materials also pose unique challenges for engineers tasked with design, analysis and certification of primary structural parts manufactured with them. In particular, two unique characteristics have been reported in [7] and [8] respectively. The open-hole tension strength of these materials was shown [7] to be virtually notch-insensitive at the macroscopic level, possibly due to the presence of internal stress concentrations arising from the heterogeneous nature of the sub-structure. This sub-structure can be identified as a meso-structure rather than a micro-structure, since it appears to be associated to the size and properties of the chips, rather than to the characteristics of the constitutive fiber and resin phases. An "inherent material" stress concentration factor was derived, and used to explain the tendency of the material to often fail at the gross-section regardless of the presence of a hole. This behavior is hole size dependent and it transitions to exclusive net-section failure for large hole sizes. Common analysis methods used for homogenous materials, independent from their orthotropic nature, cannot be used to predict notched strength load and location of failure, although it was shown that a modified Point Stress Criterion employing large characteristic length values can be used. The non-homogeneous meso-structure appears to be responsible also for the observations in [8], where axial Young's modulus measurements, conventionally obtained by strain gage or extensometer, yield up to 19% Coefficient of Variation (CoV) from specimen to specimen as well as within a single specimen. A series of tensile tests was conducted while systematically varying strain gage length, from 0.125 in. up to 2.0 in. (3.2 mm to 50.8 mm), as well as strain gage and extensometer location along the length and across the width of the specimen. Values have been measured in different locations on the same specimen that vary from as low as 3.0 Msi to as high as 9.0 Msi (20.68 GPa to 62.04 GPa). Longer strain gages do not appear to yield better results than shorter gages, and extensometer readings are not necessarily better than strain gage ones, thus suggesting that the length scale associated with these strain/ modulus variations is greater than what can be measured with a large strain gage. The use of Digital Image Correlation technique (DIC) to obtain full-field strain distributions on the surface of the specimen revealed a complex state of variable strain in the specimen, with peaks and valleys throughout the specimen. It also allowed for obtaining the most comprehensive modulus measurement by averaging the strain values over the entire surface of the tensile coupon, and thus showing that the average material modulus is indeed relatively constant with 5% CoV. These observations support that the observed variation

in local modulus are peculiar to this material, whose heterogeneous meso-structure is comprised of highly orthtropic and finite yet long reinforcements.

Proposed here is a methodology for the analysis of specimens comprised of this material, in particular for the prediction of the tensile elastic modulus. The method is based on the experimental observation that the reinforcing chips are randomly distributed, and that there is a random repeating pattern of local maxima and minima for the modulus on the surface of the specimen. This pattern can be isolated into Random Representative Volume Elements (RRVE) of random elastic characteristics. The methodology presented utilizes a randomization process that assigns elastic properties to the RRVE based on random stochastic considerations. Then it applies Classical Laminated Plate Theory (CLPT) to an equivalent quasi-isotropic tape laminate of stacking sequence based on that of the discontinuous RVE. The axial elastic modulus for the RVE is then generated for each randomization cycle, and through convergence and sensitivity studies it is shown that the predicted modulus falls well within the range of the experimental observations. The method is then validated in an application to a commercial Finite Element model, which discretizes a tensile specimen in multiple RVE regions, and assigns them randomly generated elastic properties. These RVEs, whose nodes are merged to ensure compatibility of displacements, are then solved simultaneously to yield the global mechanical response, which captures the experimentally observed variations in modulus measurements.

II. Material fabrication and test setup

All discontinuous carbon/ epoxy specimens are manufactured by Hexcel in Dublin, CA and Kent, WA utilizing HexMC. After molding, the panel is trimmed 1.0 in. (25.4 mm) on all sides to remove the regions of high flow toward the mold edges, where it is more likely that chip alignment and distortion may occur, Figure 1. Good manufacturing procedures show that the plate contains minimal number of voids or resin-starved areas. Although this is a low-flow process, unlike typical SMC molding where the charge covers only a small fraction of the mold, some degree of resin flow still takes place during the molding process. This is not sufficient to create a noticeable alignment of the fibers along any preferred direction, but inevitably lead to the formation of small resin-rich areas. Non-destructive inspection by means of pulse-echo ultrasound is used to verify the quality of the molded panel, Figure 2. C-scan images are difficult to interpret compared to tape laminates. With ultrasonic inspection, any change

in material properties, such as the presence of a defect or of a thickness transition, is characterized by attenuation in the signal. For this material form, there are point-to-point variations in material properties due to the random chip distribution, which generates signal attenuation often not corresponding to the presence of a true defect. It becomes difficult to isolate the presence of a small defect from the background noise. Through micrographic analysis of multiple regions in the molded panel has shown that the regions of signal attenuation are often not associated to macroscopic defects, and that the molded plates are generally free of defects, Figure 3. An example micrograph at 50x magnification shows the meso-structure of the laminate, comprised of chips of different cross-sectional length, stacked and oriented randomly through the thickness.

The experimental portion of this study is limited to tensile testing of two specimen geometries in the elastic region, Figure 4. All specimens are loaded conservatively to 2500-3000 microstrain, or one-fourth of the strain-to-failure of the material, in order to ensure that the behavior remains in the purely elastic region. The first geometry, referred to as the small specimen, is that of a typical tensile coupon [6-8], featuring straight-sided rectangular geometry with dimensions 10.0 in x 1.5 in (254 mm x 38 mm) and nominal thickness of 0.165 in. (4.2 mm). Since glass/ epoxy tabs of length 1.0 in. (25.4 mm) are used to grip the specimen, the effective gage length is reduced to 8.0 in. (203.2 mm), and a corresponding area of 12 in^2 (7742 mm^2).

The second geometry, referred to as the large specimen, is comprised of a straight-sided rectangular geometry with dimensions 10.0 in x 5.0 in (254 mm x 127 mm). Previous research on textile composites [9] suggests that in order to capture the behavior for material exhibiting a distinct meso-structure it is recommended to consider a test specimen size with dimensions 2.5 times the dimension of the unit-cell, or RVE. For these discontinuous materials, the large specimen is selected to be 2.5 times the length of the reinforcing chip, which has a length 2.0 in. (50.8 mm). The purpose is to identify a possible variation in measured modulus associated with the finite width of the test specimen. Since glass/ epoxy tabs of length 1.0 in. (25.4 mm) are used to grip the specimen, the effective gage length is also reduced to 8.0 in. (203.2 mm), and a corresponding area of 40 in^2 (25800 mm^2).

Modulus is measured by means of a commercial DIC system, VIC-3D by Correlated Solutions Inc. The system consists of two high-resolution cameras and an image analysis computer program capable of measuring large displacements and strains. The specimen is coated with a white spray paint, and a random pattern of black speckle

marks is applied to the surface to be analyzed. The photogrammetry system captures images of the deforming object at predefined intervals during the test and compares them, thereby constructing a real-time plot of the deformation. This system can provide unique insight in the full-field strain state of the specimens due to its non-contact and non-local nature. A more detailed discussion on the use of DIC to successfully measure full-field modulus for these discontinuous materials is presented by the authors in [8].

All specimens are loaded at a rate of 0.05 in/min. (1.3 mm/min) in a 2-grip hydraulic tension/ compression test frame. Glass/ epoxy tabs are bonded to the specimen using 3M Scotchweld film adhesive. All modulus measurements reported in the following section are the average of three independent measurements, which are run consecutively on the same specimen and in the same fashion, after ungripping, realigning, and reloading the specimen in order to guarantee repeatability. Eleven small specimens and two large specimens have been tested, as summarized in Tables I and II.

A limited set of specimens, are machined and subject to resin burn-off and de-plying, to determine the number of chips comprised with a single RVE, and their in-situ molded thickness. Burn-off temperature (850° F or 454° C) and duration (3 hours) are calibrated carefully in order to allow for partial resin burn-off while retaining sufficient chip integrity for subsequent de-plying.

III. Experimental observations

With the aid of the DIC system, it is possible to record full-field strain distribution on the surface of the specimen. Since the applied load is also recorded for every image, it is then possible to generate instantaneous multi-chromatic modulus plots such as the ones shown in Figure 5. Shown for each specimen are the maximum, minimum and average moduli recorded. It can be seen that here is a great variation in local modulus distribution, with peaks and valleys throughout the entire specimen. For both specimen sizes, these regions of high or low modulus appear to have a repeating pattern of isolated or neighboring ellipses, oriented transverse to the loading direction, and of somewhat characteristic size. This behavior has already been reported in part by the authors in [8]. The maximum, average and minimum instantaneous moduli can be plotted in the stress-strain diagrams of Figure 6, for the small specimen of Figures 4, left and 5, left. It should be noted how the difference between the average and the upper and lower bounds increases as the stress (or strain) is increased.

The results for all specimens tested are reported in Tables I and II. It should be noted that the average, maximum, minimum, and CoV values reported in the right-most column correspond to the values measured within an individual specimen. For a single specimen, denoting with E_x^i the point-measurement via DIC of the modulus in the i^{th} point on the surface of the specimen, it is possible to obtain statistical information on all point-measurements. In general, these values provide an indication of the point-to-point variation of the modulus over the surface of a single specimen:

$$\begin{aligned}
&\text{Avg } (\varepsilon_x^1, \varepsilon_x^2, \ldots, \varepsilon_x^i) \rightarrow \text{Avg } \varepsilon_x \rightarrow \text{Avg } E_x \\
&\text{Max } (\varepsilon_x^1, \varepsilon_x^2, \ldots, \varepsilon_x^i) \rightarrow \text{Max } \varepsilon_x \rightarrow \text{Max } E_x \\
&\text{Min } (\varepsilon_x^1, \varepsilon_x^2, \ldots, \varepsilon_x^i) \rightarrow \text{Min } \varepsilon_x \rightarrow \text{Min } E_x \\
&\text{Stdev } (E_x^1, E_x^2, \ldots, E_x^i) \rightarrow \text{Stdev } \varepsilon_x \\
&\text{CoV}^{\text{specimen}} = \text{Stdev } \varepsilon_x / \text{Avg } \varepsilon_x
\end{aligned} \tag{1}$$

The average, maximum, minimum, and CoV values reported at the bottom of Tables I and II apply to the average measured E_x values across all specimens. Among all specimens, it is possible to draw statistical considerations regarding the specimen-to-specimen variation of the average values of E_x. Denoting with $\text{Avg } E_x^i$ the average modulus of the j^{th} specimen, we can write:

$$\begin{aligned}
&\text{Avg } (\text{Avg } E_x^1, \text{Avg } E_x^2, \ldots, \text{Avg } E_x^j) \rightarrow \text{Avg } (\text{Avg } E_x) \\
&\text{Max } (\text{Avg } E_x^1, \text{Avg } E_x^2, \ldots, \text{Avg } E_x^j) \rightarrow \text{Max } (\text{Avg } E_x) \\
&\text{Min } (\text{Avg } E_x^1, \text{Avg } E_x^2, \ldots, \text{Avg } E_x^j) \rightarrow \text{Min } (\text{Avg } E_x) \\
&\text{Stdev } (\text{Avg } E_x^1, \text{Avg } E_x^2, \ldots, \text{Avg } E_x^j) \rightarrow \text{Stdev } (\text{Avg } E_x) \\
&\text{CoV}^{\text{averages}} = \text{Stdev } (\text{Avg } E_x) / \text{Avg } (\text{Avg } E_x)
\end{aligned} \tag{2}$$

It can be seen in Tables I and II that the CoV observed within a specimen, $\text{CoV}^{\text{specimen}}$ (eq. 1) is as high as 19%, which is similar to the CoV reported by the authors in [8] and corresponding to the kind of error that would be obtained if a point-measurement were to be performed using a strain gage. On the other hand, the CoV across the average specimen moduli, $\text{CoV}^{\text{averages}}$ (eq. 2) is much more consistent across multiple specimens and is less than 5%. This observation suggests that the material is highly heterogeneous on a local basis, but the manufacturing process employed is consistent since the average variation from specimen to specimen is very low. The results obtained for the large specimens, Table II, seem to show an extremely low value of $\text{CoV}^{\text{averages}}$. However, due to the limited

number of large specimens available for testing it is difficult to extrapolate statistical considerations. Nonetheless, the importance of testing the large specimens will become clear in the next sections.

The unidirectional tape from which the chips are derived has axial and transverse moduli E_1 = 16.5 Msi (113.7 GPa) and E_2 = 1.22 Msi (8.41 GPa). These constitute the upper and lower bounds respectively for the discontinuous material. If at a generic point on a specimen the chips were to be all oriented in the 0° direction, the DIC would measure an $E_x = E_1$, while if at another point all the chips were oriented in the 90° direction, then it would measure an $E_x = E_2$. Experiments conducted show that the maximum recorded modulus for the small tensile specimen (Table I) is only 10.3 Msi (71.0 GPa), while the minimum is 3.02 Msi (20.8 GPa). This means that since there are approximately 30 chips through the thickness of the laminate thickness considered (see Figure 3), the probability of having all chips at one point in the specimen oriented in the 0° or 90° direction is minimal.

If a path line is plotted on a DIC specimen, it is possible to obtain the strain (hence modulus) variation along such path, Figure 7. The path shows the strain profile plotted against the normalized axial position. In the plot the center straight line corresponds to the average strain (hence average modulus) recorded on the specimen. The other two lines correspond to an upper and a lower bound of ±20% of the average strain. These lines can be thought of as a filter that is used to isolate the regions of high or low strain that exceed the average strain by at least 20%. The reason to adopt this strategy is to eliminate any "noise" associated with the measurement. The strains comprised between the bounds are considered to be sufficiently near the average to be smeared together with the average strain. If this "filtering" scheme is used, it is then possible to use a tri-chromatic plot, for which one color is assigned to the regions of +20% strain, another color to the regions with –20%strain, and one for the average strain regions. The regions of become more distinct and it is possible to quantify the size of the peaks and valleys. It should be remembered that a region of high strain corresponds to a region of low modulus, and vice versa. As an example, we can apply this procedure to a generic multi-chromatic DIC region, shown in Figure 8 (top). If we plot the strain distribution along a horizontal path line in the middle of the region, we obtain the profile in Figure 8 (center). It is then possible to draw the line corresponding to the average specimen strain, and the two lines corresponding to the ±20% bounds. The region of peak strain can be isolated from the average strain, and its size becomes clearly defined, Figure 8 (bottom).

Using this "filtering" scheme to the two specimens of Figures 4 and 5, it is possible to obtain the tri-chromatic distributions of Figure 9. These distributions that the regions of high or low strain appear to have an elliptical shape of average area 0.212 in^2 (136.8 mm^2) and 0.317 in^2 (204.5 mm^2) for the small and large specimens respectively, as measured by image analysis. This yields an average area of 0.262 in^2 (169 mm^2). Because of the random and heterogeneous meso-structure of this material, it is not possible to identify a self-similar repetitive pattern, such as the Representative Volume Element (RVE) used in micromechanical analysis of unidirectional tape, fabric or textile composites. However, it is possible to define a characteristic area or characteristic length scale for these regions of high or low strain. These regions have random material properties, locations and distributions, but exhibit a repetitive pattern in their randomness. Therefore we shall make the leap of faith as to call these regions Random Representative Volume Elements (RRVE).

Based on these considerations, it is possible to proceed to identify the micro- or meso-structure of the material contained within an RRVE. Since it is difficult to machine an elliptical shape of exactly 0.262 in^2 (169 mm^2) from a molded panel, a square coupon of dimensions 0.5 in. x 0.5 in. (12.7 mm x 12.7 mm), corresponding to an RRVE area of 0.250 in^2 (161 mm^2) is machined. These specimens are then subject to resin burn-off inside a furnace, and then de-plied chip-by-chip, as shown in Figure 10. The chips are then dispersed flat on a surface for subsequent image analysis to calculate the total chip area $\sum A_i^c$ within the selected RVE, as summarized in Table IV. For the conservation of mass and volume, we can write the following expression:

$$\left(\sum A_i^c\right) \cdot t^c = A^{RVE} \cdot t \tag{3}$$

where t^c is the equivalent chip thickness, A_i^c is the area of a i^{th} chip fraction, contained in the RRVE, A^{RVE} and t are the surface area and thickness of the RVE. Since A^{RVE} = 0.250 in^2 (161 mm^2) and t = 0.165 in. (4.2 mm). The quantity t^c can be determined, and it corresponds to the thickness of a single chip after cure, and the average in-situ value thus calculated 0.00495 in. (0.126 mm), very close to the nominal cured tape prepreg thickness of 0.005 in. (0.127 mm). This investigation is fundamental to understand that within a given volume of material, the size of chips varies anywhere from a nearly intact chip to negligible fractions of chips. Hence it establishes the confidence that both chip size and orientation within a given RRVE is random.

IV. Randomization Algorithm and Laminate Analogy

The foundation of the modeling strategy proposed here is the laminate analogy for discontinuous fibers proposed by the co-author in Halpin and Pagano [2]. The laminate analogy proposes that the macroscopic elastic properties of a two-dimensional randomly oriented short fiber plate can be predicted based on the properties of a quasi-isotropic $[0/90/\pm45]_s$ laminated plate of aligned short fibers of identical volume fraction and aspect ratio, Figure 11. With such approach, it is the possible to use Classical Laminated Plate Theory (CLPT) to predict, for example, the axial modulus E_x for a random discontinuous fiber composite.

The method proposed here is a modified laminate analogy, since it is based on the analogy between the quasi-isotropic discontinuous fiber plate (the physical plate) and a quasi-isotropic laminated plate of continuous fibers (the equivalent laminate), Figure 12. The properties of the equivalent laminate are determined through a stochastic process, which, based on a set of input properties of the physical plate, generates a random distribution of sizes and orientations for the chips of the physical plate. One randomization run for the physical plate generates one equivalent laminate. For multiple randomization runs, multiple equivalent laminates of different ply distributions, hence elastic properties, are generated. This process is outlined in Figure 13 and will be explained in detail later.

From the discontinuous fiber plate (the physical plate), the input properties required for the code are:

- Measurement window area and thickness
- Nominal chip area
- Equivalent chip thickness
- Number of possible chip orientations

The measurement window is the portion of the physical laminate being considered, and hence it is a measure of the number of chips, or portions of chips, being included in the analysis. The thickness of the measurement window t^{mw} is kept constant throughout the study, and it corresponds to the plate thickness t = 0.165 in. (4.2 mm). The area of the measurement window A^{mw} is varied to identify the sensitivity of the analysis to the number of chips being considered. It is also used to verify analytically the experimental observations reported in [8], concerned with the differences in local measurements (such as strain gages) and full-field measurements (DIC). The area of the measurement window varies between the following values, Table IV:

- 0.062 in^2 (40 mm^2) – corresponding to a 0.25-in. (6.35 mm) strain gage

- 0.25 in^2 (161 mm^2) – corresponding to the square RRVE
- 2.0 in^2 (1290 mm^2) – corresponding to one-quarter section of a the surface of a small tension specimen
- 12.0 in^2 (7742 mm^2) – corresponding to the full area of the small specimen
- 40.0 in^2 (25800 mm^2) – corresponding to the full-field area of the large specimen

The nominal chip area A^c is kept constant at 0.66 in^2 (426 mm^2) throughout the study, and corresponds to the physical area of a single chip of dimensions 2.0 in. x 0.33 in. (50.8 mm x 8.4 mm). The equivalent chip thickness t^c is kept constant and is equal to 0.00495 in. (0.126 mm) as determined experimentally in the previous section.

The number of possible chip orientations *n* indicates all the possible angles θ_i that a chip can attain. Theoretically, an infinite number of orientations between 0 and 180 degrees are possible. However, in this study, the number of orientations allowed is varied between n = 4, 8, 16, and 32. This in turn corresponds to allowing the relative increment between orientations to be $\frac{\pi}{n}$, or 45°, 22.5°, 11.25°, 5.625° respectively. For example, for n = 8, hence $\frac{\pi}{8} = 22.5$, and the following angles are possible: $\theta_1 = 0$, $\theta_2 = +22.5$, $\theta_3 = +45$, $\theta_4 = +67.5$, $\theta_5 = 90$, $\theta_6 = +112.5 = -67.5$, $\theta_7 = +135 = -45$, $\theta_8 = +157.5 = -22.5$.

A randomization algorithm developed using Matlab assigns to each chip fraction a random size and a random orientation. A "while" loop initiates, which adds a fraction of chip k_j, which can have any value between [0, 1]. The orientation is randomly assigned among all possible orientations. The Matlab command used is 'rand', which returns a scalar value drawn from a uniform distribution on the unit interval.

For each possible orientation, as specified in the input, the oriented chip area $A(\theta_i)$ corresponds to the sum of all chip areas at the given orientation. This process is repeated until the total volume of fractions of chips reaches the volume of the measurement window. Once it is reached, the code stops adding chips. This is expressed as:

$$t^{mw} \cdot A^{mw} = t^c \cdot \left[A(\theta_1) + \ldots + A(\theta_i) + \ldots + A(\theta_n)\right] \tag{4}$$

where the nomenclature has been previously defined and

$$A(\theta_i) = A^c \cdot \sum (k_j)_{(\theta_i)} \tag{5}$$

The assumption that fractions of chips, rather than full chips only, should be considered is based on the experimental observation that the size of the chips contained in a volume of material comprises small and large portions of chips, Figure 10. The assumption that the distribution of sizes is random is also justified by experimental observations [6-8], Figure 3.

At the end of the randomization algorithm, the code then proceeds to calculate the properties of the virtual laminate. This is a balanced, symmetric continuous fiber tape laminate of the form $\left[0/\pm\frac{\pi}{n}/\pm\frac{2\pi}{n}/.../90\right]_s$. The possible ply orientations of the equivalent tape laminate are the same as the possible chip orientations. The thickness of a ply along each orientation in the tape laminate is proportional to the fraction of chips at the same orientation in the discontinuous plate. This is expressed as:

$$t_c \cdot \sum A(\theta_i) = 2 \cdot t_{\theta i} \cdot A^{mw} \tag{6}$$

This expression is again based on the conservation of mass/ volume. For the n = 8 case, the following thicknesses are determined: t_0, $t_{\pm 22.5}$, $t_{\pm 45}$, $t_{\pm 67.5}$, t_{90}. In general, the ply thicknesses for each orientation are different from each other, and are fractions of numbers (not integers). It should be noted that they do not represent a physical ply thickness. They are virtual thickness of an equivalent tape laminate that has the same fraction of fibers aligned along a certain orientation as the discontinuous (physical) plate. The factor of 2 on the right hand side of eq. 6 comes form the fact that the laminate is symmetric.

The unidirectional tape properties (E_{11}, E_{22}, G_{12} and ν_{12}.) are then used as input to the code. It should be noted that these properties are the true elastic properties of both the individual chip (in the physical plate) and of the unidirectional tape ply (in the virtual laminate). Hence, for this class of materials, the analogy between the physical plate and the virtual laminate is extremely consistent.

At the end of the randomization algorithm and laminate analogy process, the Matlab code generates as outputs the thicknesses of the plies at each possible orientation for the equivalent tape laminate. The elastic properties of the tape laminate can be then predicted through the use of a standard laminate code. Using CLPT, the average axial modulus E_x for the measurement window is calculated as that of a symmetric, balanced laminate:

$$E_x = \frac{1}{t}\left(A_{xx} - \frac{A_{xy}^2}{A_{yy}} \right) \tag{7}$$

where the A_{ij} terms represent the terms of the A matrix.

This completes a single run of the analysis code, which takes a few milliseconds on a desktop computer. For a single run, the predicted value has been observed to fall anywhere in the range 3.0-10.0 Msi (20.7-68.9 GPa). In order to obtain statistical distribution of these predictions, the code is run multiple times, and for each run the value of E_x is recorded. This process is summarized in the flowchart of Figure 13.

V. Example input-output

Example input (US customary units of in., lb, Msi):

$A^{mw} = 12.0$ in.^{2}, $t^{mw} = 0.165$ in.	#measurement window Area and thickness#
$A^c = 0.66$ in.^{2}, $t^c = 0.00495$ in.	#single chip area and thickness#
n = 4	#number of possible chip orientations#
runs = 5,000	#number of algorithm cycles to be repeated#
$E_{11} = 16.5$ Msi, $E_{22} = 1.22$ Msi, $G_{12} = 0.6$ Msi, $\nu_{12} = 0.309$	#tape lamina elastic properties#

For the i^{th} run of the algorithm:

Possible orientations: $\theta_1 = 0$, $\theta_2 = +45$, $\theta_3 = -45$, $\theta_4 = 90$

While loop begins – adds random fractions of chips k_j at each random orientation θ_i:

0	±45	90
0.321	0.023	0.001
0.622	0.112	0.646
…	…	…

The quantities below are generated:

$$\left\{\begin{array}{l} A(0) = A_c \cdot \sum\left[k_j(0)\right] = 0.66 \cdot \left[0.321 + 0.622 + ...\right] = 247.3\ in.^2 \\ A(\pm 45) = A_c \cdot \sum\left[k_j(\pm 45)\right] = 0.66 \cdot \left[0.023 + 0.112 + \ ...\right] = 83.4\ in.^2 \\ A(90) = A_c \cdot \sum\left[k_j(90)\right] = 0.66 \cdot \left[0.001 + 0.646 + ...\right] = 69.3\ in.^2 \end{array}\right\}$$

The while loop ends when the condition below is satisfied:

$$\frac{t^{mw} \cdot A^{mw}}{t^c} = 400\ in.^2 = \left[A(0) + A(\pm 45) + A(90)\right]$$

With ply percentages are:

$$\left\{\begin{array}{l} \%0 = \dfrac{247.3}{400} = 0.618 = 61.8\% \\ \%\pm 45 = \dfrac{83.4}{400} = 0.208 = 20.8\% \\ \%90 = \dfrac{69.3}{400} = 0.173 = 17.3\% \end{array}\right\}$$

Example output:

$$\left\{\begin{array}{l} t_0 = \dfrac{1}{2} \cdot 0.618 \cdot 0.165 = 0.0510\ in. \\ t_{+45} = \dfrac{1}{4} \cdot 0.208 \cdot 0.165 = 0.0085\ in. \\ t_{-45} = \dfrac{1}{4} \cdot 0.208 \cdot 0.165 = 0.0085\ in. \\ t_{90} = \dfrac{1}{2} \cdot 0.173 \cdot 0.165 = 0.0143\ in. \end{array}\right\}$$

These are the ply thicknesses for the equivalent laminate, an 8-ply quasi-isotropic $[0/+45/-45/90]_s$. It is noteworthy that a laminate with these ply orientations would not be quasi-isotropic for equal-ply thickness.

A standard laminate code is used to calculate the ABD matrix for the above laminate, and the elastic modulus of the laminate is computed. In this case, E_x = 11.3 Msi (77.9 GPa). The code then records and stores this value, then proceeds to repeat the randomization algorithm to generate the virtual ply thicknesses for a different equivalent tape laminate.

VI. Sensitivity study

The analysis method described is repeated over multiple runs, specifically 1-10-100-500-1,000-5,000-10,000-15,000 and 20,000. Even for the higher number of runs, the code takes only a few seconds to run on a desktop computer. As previously discussed, the unidirectional tape lamina moduli E_1 and E_2 constitute the upper and lower bounds respectively that the E_x of the discontinuous plate can attain at any point. Theoretically, a single randomization algorithm could generate predicted E_x values as high as E_1 and as low as E_2 for a selected measurement window and number of possible orientations. It is necessary to obtain a statistically relevant distribution for the predicted values by running the algorithm multiple times. The predicted distribution for 10, 100 and 1,000 runs is shown in Figure 14, where the abscissa is the normalized number of runs (in values of %). The number of possible orientations is 8 and the measurement window area is that of the RRVE. It can be seen that for 10 runs, the distribution tends to be coarse and to slightly underestimate the maximum and minimum values of E_x. For 1,000 runs, the distribution is very uniform and continuous, and the maximum and minimum moduli predicted are well defined. In general, average E_x values appear to be quite insensitive to number of runs. It can be seen that, for an RRVE, the maximum and minimum values of E_x calculated in a single randomization run, over as many as 20,000 runs, are far lower and greater respectively than the maximum E_1 and minimum E_2 of the unidirectional tape (Figure 14). This in turn confirms that the probability that the random distribution of approximately 30 chips through the specimen thickness is oriented all in the 0 or the 90 directions is extremely limited.

For a full-size small tensile specimen, the predicted maximum, minimum and average E_x are shown to converge asymptotically after 5,000 runs in Figure 15. The CoV for the distribution is also relatively stable with number of runs, at approximately 3%. In general, it can be observed from Figures 14 and 15 that the statistical distribution of the random predicted E_x converges relatively quickly to consistent E_x maximum, minimum and average values. Also, predicted values are in good agreement with experimental observations through strain gage, extensometer and DIC.

The number of possible orientations is a key input to the randomization and laminate analysis code, and has been arbitrarily varied between 4 and 32, as discussed previously. A sensitivity study shows that the average, maximum and minimum predicted E_x values are insensitive to this parameter in the range 4-32. This means that as long as the

chopped plate or the equivalent tape laminate have at least four principal directions (that is, at 45 degree increments) the predicted values do not vary over the number of cycles (5,000 are used to generate the plot of for Figure 16). However, for n = 2, hence for a cross-ply laminate comprised of only 0 and 90 degree plies, predictions are highly inaccurate.

A key input to the randomization and laminate analysis code is the measurement window area. Numerically, this value dictates the amount of discontinuous material, hence the amount of random chips, among which randomization the randomization process takes place. Physically, it indicates the size of surface area that is observed through DIC. As discussed before, this value can be as small as the footprint of a small strain gage, the size of the square RRVE, or as large as a full-field DIC area of a tensile specimen. Key values of the measurement window areas are reported in Table V, together with the experimentally determined and predicted maximum, minimum, average and CoV values of E_x. The data is generated for a baseline of 5,000 runs and 8 possible orientations.

It can be seen that there is a strong dependence of all predictions on the area of the measurement window, consistently with experimental observations, Figure 17. Predicted values are in good agreement with experimental observations reported by the authors in [8] for strain gage measurements over multiple locations on the same specimen. Since the motivation of this study is to capture analytically the variability of E_x observed experimentally, Figure 18 shows the details of the CoV distribution previously shown in Figure 17, top. It can be seen once again that the measured variation decreases sharply with increasing measurement window area, from as high as 18% to an asymptotic value between 2-4%. Superimposed are the average values obtained experimentally by the authors with strain gages in [8] and through DIC in this study (Tables I and II). It can be seen that the predictions are in good agreement with all experimental results.

VII. Application to a Finite Element model

Once the proposed approach has been checked to ensure convergence and has been validated against experimental data, it is possible to apply it to any subsequent analysis procedure. In this study, the analysis approach is applied to a Finite Element (FE) model of a small specimen under uniaxial tension. The idea is to reproduce with the aid of a commercial FE code (ANSYS) the experimental observations on the small tensile specimen. Specimen

dimensions are 12.0 in. x 1.5 in. (304.8 mm x 38.1 mm). The specimen is subdivided into square regions of size 0.5 in. x 0.5 in., corresponding to the 0.25 in.^{2} (161.3 mm^2) RRVE determined experimentally in the previous sections. Each RRVE is assigned orthotropic material properties independently from the neighboring RRVE. There are a total of 48 RRVE on a single specimen, Figure 19. The discretization of the specimen into RRVE bears no relationship to mesh size, as discussed later. The properties for each RRVE are generated by running once the stochastic laminate analogy code discussed previously; hence, for a full specimen, 48 runs are needed. The code is designed to interface directly with the FE software; hence, the Matlab output feeds directly as input to the ANSYS model.

The Shell99 element in ANSYS is used in this model, which is a linear layered structural shell, and it allows for assigning individual ply thicknesses, which are obtained from the stochastic laminate analogy code. Each RRVE is meshed, and the nodes of neighboring are merged to ensure displacement compatibility. Three mesh sizes have been used to asses the sensitivity of the modeling approach to element size, Figure 20. The number of elements varies from 192, 768, to 3072, corresponding to 4, 16, and 64 elements per RRVE. All degrees of freedom are constrained on the outermost left line of nodes, corresponding to the fixed test grip, while an axial displacement of 0.1 in. (2.54 mm) is applied to the outermost right line of nodes, corresponding to the moving grip.

Solution takes only a few seconds on a desktop computer. The contour plot for the nodal solutions of the principal strain in the axial direction is shown in Figure 21. The distribution of strain with peaks and valleys is similar to the experimentally observed distributions of Figure 5, left. The corresponding maximum, minimum, average and CoV of E_x are obtained using the load calculated from the reaction forces and the boundaries, and are reported in detail in Table VI. For a single FE run of one small tensile specimen, the $CoV^{specimen}$ is approximately 10%, consistent with the experimental observations and the stochastic algorithm predictions for the 12 in.^{2} (7,742 mm^2) measurement window area, Tables I and V. If the FE model is run multiple times, a statistical averaging of the average E_x values can be obtained, and the the $CoV^{averages}$ decreases. For 10 Finite element runs, corresponding to 480 algorithms runs, the CoV of the average E_x is approximately 2%. Mesh density seems to have little effect on the predicted maximum, minimum and average values of E_x, as reported in Table VI. The surface strain distribution for the coarse, medium and fine mesh densities remains relatively constant as well, as shown in Figure 22 for another run of the FE code. However, for increasing number of elements, hence for smaller element sizes, the discontinuity

at the regions' boundaries appears sharper. The situation improves if the smoother element solution were to be plotted rather than the nodal solutions.

In general, it is shown that the stochastic laminate analogy analysis method proposed, based on the random generation of elastic properties for repeating random material unit cells, can be applied to successfully capture the macroscopic mechanical behavior for this class of materials.

VIII. Immediate relevance and future research

The proposed methodology can be used within the context of an allowables-based certification methodology, also known as certification by analysis supported by test evidence. To validate analysis models, certification test article are typically strain-gaged and strain surveys are taken at critical load values, such as design limit load (DLL) [10]. If the strain measured at the strain gages at DLL correlates with the value predicted by the analysis tool in that location, the validation is considered successful. It should be noted that for current regulatory agency requirements, the component must remain in its linear elastic region up to DLL and not exhibit damage growth. For components manufactured with these new material forms, it has been shown [8] that strain gages cannot be used accurately to measure the material's global modulus, and the point-measurements obtained via strain gage can differ greatly based on the random mesostructure. Hence DLL model validation using the conventional approach becomes very difficult, if not impossible. Full-field strain measurement techniques, such as DIC, have the potential to provide the global strain survey response needed from the experimental standpoint, but analytically the models cannot capture the variation. A probabilistic approach, such as the proposed one, can be used to generate statistical average predictions of the strain distributions, which can be then correlated with the experimental results. In the current commercial aircraft industry, Margin of Safety (MoS) calculations, such as static strength and stability/ crippling are based on modified maximum strain failure criterion applied at the laminate level [11]. The material is assumed to be linear and elastic up to failure and the nominal value of modulus is used to calculate the allowable value. Currently-accepted deterministic analysis models cannot be employed for these new material forms, and hence it is important that a probabilistic approach be embraced. This methodology, which is capable of capturing the random variation in the local stress field, has also the potential to offer insight in the complex effects of stress concentrations and the apparent notch insensitivity of this class of materials, reported in [7].

The proposed stochastic methodology will be adapted to the prediction of first-ply failure strength and ultimate laminate failure strength. Since shear stress transfer is particularly important for discontinuous fiber composites, there is a possibility that for these materials first ply failure (i.e. matrix failure in the 90º chips) may be responsible for complete laminate failure (i.e. coincide with fiber failure in the 0º chips). It is possible that lamina-based failure criteria, such as Tsai-Wu, may be well suited to predict part performance for this type of discontinuous fiber composites.

IX. Conclusions

A new material form is being considered for aircraft primary structural applications, and consists of discontinuous carbon fiber/ epoxy random mat of chopped unidirectional prepreg tape. Commercial applications for this type of material form already exist, such as Hexcel HexMC®. Previous studies by the authors have shown that these materials exhibit variation in elastic modulus that is greater than the variation observed in the strength, and as high as 20%. These observations have been reported both via strain gage and extensometer measurements, and confirmed by full-field strain measurements via Digital Image Correlation This variation is attributed to the highly non-homogenous meso-structure of the material, comprised of highly orthotropic chips of discrete dimensions. With the aid of a full-field strain measurement on a full-size tensile specimen, the measured CoV is as low as 5%, thus suggesting that the average material properties are very consistent over large regions. Since traditional analysis methods used for continuous fiber composites do not account for local variations in elastic properties of the material, an analysis method is proposed here to account for the local variation in elastic modulus. Based on experimental observations, a Random Representative Volume Element (RRVE) is established. The randomly-distributed chips contained in it are idealized as a balanced, symmetric tape laminate of equivalent surface area. A stochastic process is used to generate statistical distributions for the fraction and orientation of plies for this laminate, which is then analyzed via Classical Laminated Plate Theory. For each run, the predicted axial elastic modulus is calculated. Based on multiple runs, a statistical distribution of modulus predictions is obtained, and the maximum, minimum, and average E_x values, as well as CoV are consistent with experimental observations. A parametric study shows that the algorithm converges to asymptotic values with relatively few runs, and highlights the method's sensitivity to measurement window area. An example use of this method has been shown as it applies to model a tensile coupon with a commercial Finite Element Model. The model discretizes the coupon in multiple RRVE, having elastic

orthotropic material properties assigned independently from the neighboring ones and generated by running the stochastic laminate analogy code. The regions are connected by merging nodes, and then solved simultaneously. The proposed randomization algorithm in conjunction with the laminate analogy yields predictions that are in excellent agreement with experimental observations, and seems to indicate that statistical averaging of stochastic distributions is capable of capturing the variability in the mechanical behavior for these materials.

Acknowledgments

The research was funded through the JAMS/ AMTAS program with matching funds from FAA and Boeing, and in-kind support of materials and parts from Hexcel. The authors wish to acknowledge Curt Davies and Dr. Larry Ilcewicz (Chief Scientist for Composites, Federal Aviation Administration), Dr. Bill Avery (The Boeing Co., Structures Technology), Bruno Boursier and Dave Barr (Hexcel) for monitoring the progress of the research.

References

[1]Halpin, J.C., Stiffness and expansion estimates for oriented short fiber composites. Polymer Engineering and Science. 3, 1969, p.732.

[2]Halpin, J.C., Pagano, N.J., "The Laminate Approx. for Randomly Oriented Short Fiber Composites", Polymer Engineering and Science, Vol. 3, 1969, p. 720.

[3]Kardos, J.L., Michno, M.J., Duffy, T.A., "Investigation of High Performance Short Fiber Reinforced Plastics", Final Report, Naval Air Systems Command, No. N00019-73-C-0358, 1974.

[4]"Boeing 787 features composite window frames", Reinforced plastics, Application News, Vol. 51, Issue 3, March 2007, page 4.

[5]Porter, J., "Moving closer to the goal of cost effective complex geometry carbon composite parts", HPC4HPC Special Session, Proceedings of the 19th ASC Technical Conference, Atlanta, GA, Sept. 2004.

[6]Feraboli, P., Peitso, E., Deleo, F., Cleveland, T., Stickler, P.B., "Characterization of prepreg-based discontinuous carbon fiber/ epoxy systems: Part I", J. Reinf. Plastics and Composites, 28/10, 2009, pp. 1191-1214.

[7]Feraboli, P., Peitso, E., Cleveland, T., Stickler, P.B., Halpin, J.C., "Notched behavior of prepreg-based discontinuous carbon fiber/ epoxy systems", Composites Part A, 40/3, 2009, pp. 289-299.

[8]Feraboli, P., Peitso, E., Cleveland, T., Stickler, P.B., "Modulus Measurement for prepreg-based discontinuous carbon fiber/ epoxy systems", J. of Composite Materials, 43/19, 2009, pp. 1947-1965.

[9]Poe, C.C., Dexter, H.B., Raju, I.S., "A review of the NASA textile composite research", 38th AIAA Structures, Structural Dynamics and Materials Conference, Paper No. 97-1321, Orlando, FL, 1997.

[10] Kan, H.P., Cordero, R., Whitehead, R.S., "Advanced certification methodology for composite structures", DOT/FAA/AR-96/111, April 1997

[11]Feraboli, P., "Static strength determination of laminated composite materials within the current certification methodology for aircraft structures" – Journal of Aircraft, 46/4, 2009, pp. 1365-1374.

Tables and Figures

Table I: Axial modulus DIC results for small specimens

Specimen	Avg E_x specimen Msi (GPa)	Max E_x specimen Msi (GPa)	Min E_x specimen Msi (GPa)	CoV E_x specimen (%)
1	6.27 (43.2)	9.05 (62.3)	4.17 (28.7)	13.1
2	5.57 (38.4)	7.17 (49.4)	4.64 (32.0)	11.7
3	5.92 (40.8)	7.97 (54.9)	3.02 (20.8)	18.9
4	5.69 (39.2)	8.86 (61.1)	3.95 (27.2)	13.7
5	5.88 (40.5)	7.60 (52.4)	4.56 (31.4)	9.1
6	5.74 (39.6)	8.79 (60.6)	3.96 (27.3)	17.3
7	6.28 (43.3)	10.30 (71.0)	4.59 (31.6)	13.8
8	6.29 (43.4)	9.81 (67.6)	4.27 (29.4)	12.9
9	6.09 (42.0)	8.49 (58.5)	3.93 (27.1)	15.3
10	5.69 (39.2)	9.06 (62.5)	3.89 (26.8)	16.6
11	6.23 (42.9)	8.38 (57.8)	4.29 (29.6)	12.3
Avg (Avg E_x, Max E_x, Min E_x, CoV E_x)	**5.97 (41.2)**	**8.68 (59.8)**	**4.12 (28.4)**	**14.1**
Avg (Avg E_x)	**5.97 (41.2)**	**-**	**-**	**-**
Max (Avg E_x)	**6.29 (43.4)**	**-**	**-**	**-**
Min (Avg E_x)	**5.57 (38.4)**	**-**	**-**	**-**
CoV (Avg E_x)	**4.6**	-	-	**-**

Table II: Axial modulus DIC results for large specimens

Specimen	Avg E_x specimen Msi (GPa)	Max E_x specimen Msi (GPa)	Min E_x specimen Msi (GPa)	CoV E_x specimen (%)
1	6.75 (46.5)	10.50 (72.4)	4.90 (33.8)	19.1
2	6.81 (46.9)	9.20 (63.4)	4.99 (34.4)	16.1
Avg (Avg E_x, Max E_x, Min E_x, CoV E_x)	**6.78 (46.7)**	**9.85 (67.9)**	**4.95 (34.1)**	**17.6**
Avg (Avg E_x)	**6.78 (46.7)**			
Max (Avg E_x)	**6.81 (46.9)**	**-**	**-**	**-**
Min (Avg E_x)	**6.75 (46.5)**	**-**	**-**	**-**
CoV (Avg E_x)	**0.6**	-	-	**-**

Table III: Areas of DIC regions of modulus exceeding ±20% of the average specimen modulus, for the two specimens shown in Figure 9 – units of $in.^2$ (mm^2).

Number of regions	Small tensile specimen	Large tensile specimen
1	0.151 (97.4)	0.902 (581.9)
2	0.119 (76.8)	0.142 (91.6)
3	0.237 (152.9)	0.436 (281.3)
4	0.058 (37.4)	0.074 (47.7)
5	0.29 (187.1)	0.462 (298.1)
6	0.416 (268.4)	0.117 (75.5)
7	-	0.276 (178.1)
8	-	0.019 (12.3)
9	-	0.024 (15.5)
10	-	0.142 (91.6)
11	-	0.593 (382.6)
12	-	1.077 (694.8)
13	-	0.272 (175.5)
14	-	0.055 (35.5)
15	-	0.467 (301.3)
16	-	0.449 (289.7)
17	-	0.247 (159.4)
18	-	0.221 (142.6)
19	-	0.04 (25.8)
Average	**0.212 (136.8)**	**0.317 (204.5)**

Table IV: Burn-off and de-plying results

	Nominal Dimensions in. (mm)	**t^c in. (mm)**
1	0.500 x 0.500 x 0.165 (12.7 x 12.7 x 4.2)	0.00499 (0.13)
2	0.500 x 0.500 x 0.165 (12.7 x 12.7 x 4.2)	0.00491(0.12)

Table V. Predicted vs. experimental moduli for several measurement window sizes

Measurement window #	**Experim. vs. predicted**	**A^{mw} in^2 (mm^2)**	**Avg E_x Msi (GPa)**	**Max E_x Msi (GPa)**	**Min E_x Msi (GPa)**	**CoV E_x (%)**
mw1	EXP 0.5-in. strain gage	0.062 (40)	5.96 (41.1)	7.70 (53.1)	3.75 (25.9)	15.4
	PREDICTED	0.062 (40)	6.33 (43.6)	10.20 (70.3)	3.02 (20.8)	16.1
mw2	EXP 0.5 in. x 0.5-in. RRVE	0.25 (161)	5.72 (39.4)	7.56 (52.1)	4.33 (29.8)	13.8
	PREDICTED	0.25 (161)	6.36 (43.8)	9.85 (67.9)	3.29 (22.9)	15.2
mw3	EXP 1/4 section of small tensile specimen	2.00 (1,290)	6.04 (41.6)	6.99 (48.2)	4.85 (33.4)	8.5
	PREDICTED	2.00 (1,290)	6.39 (44.0)	8.09 (55.8)	4.60 (31.7)	7.8
Mw4	EXP small tensile specimen, from Table I	12.0 (7,742)	5.97 (41.2)	6.29 (43.4)	5.57 (38.4)	4.6
	PREDICTED	12.0 (7,742)	6.40 (44.1)	7.17 (49.4)	5.64 (38.9)	3.1
mw5	EXP large tensile specimen, from Table II	40.0 (25,806)	6.78 (46.7)	6.81 (46.9)	6.75 (46.5)	0.6
	PREDICTED	40.0 (25,806)	6.39 (44.0)	6.76 (46.6)	6.00 (41.4)	1.7

Table VI: Variation in predicted modulus values as function of mesh size, for a single FEA run of the small tensile specimen

Mesh	**Avg Ex specimen Msi (GPa)**	**Max Ex specimen Msi (GPa)**	**Min Ex specimen Msi (GPa)**	**CoV Ex specimen (%)**
Coarse	6.46 (44.5)	8.48 (58.5)	4.32 (29.8)	9.8
Medium	6.46 (44.5)	8.61 (59.4)	4.30 (29.6)	10.4
Fine	6.46 (44.5)	8.64 (59.6)	4.24 (29.2)	10.8

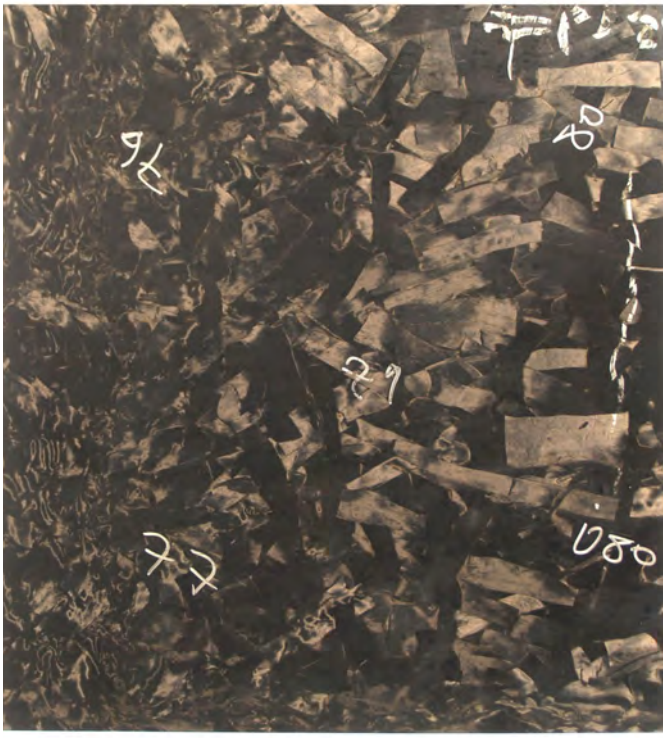

Figure 1. Molded and trimmed panel

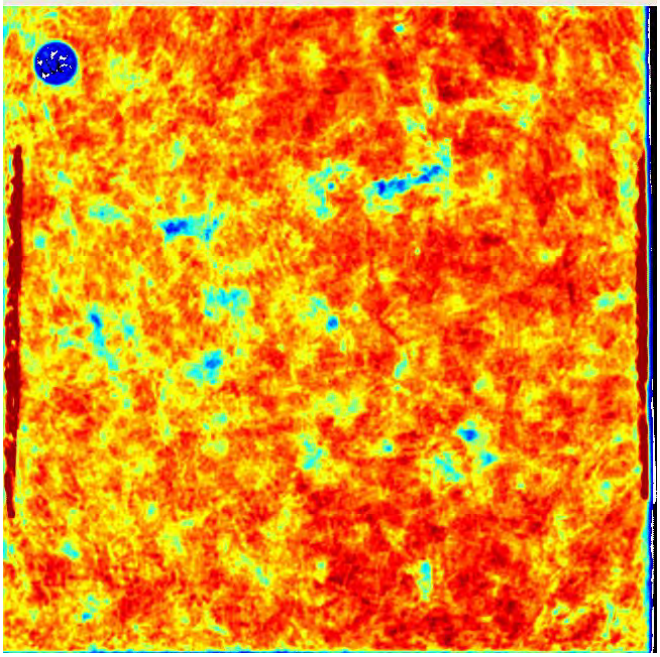

Figure 2. C-scan pulse-echo ultrasonic image of a molded panel using a 5 MHz sensor.

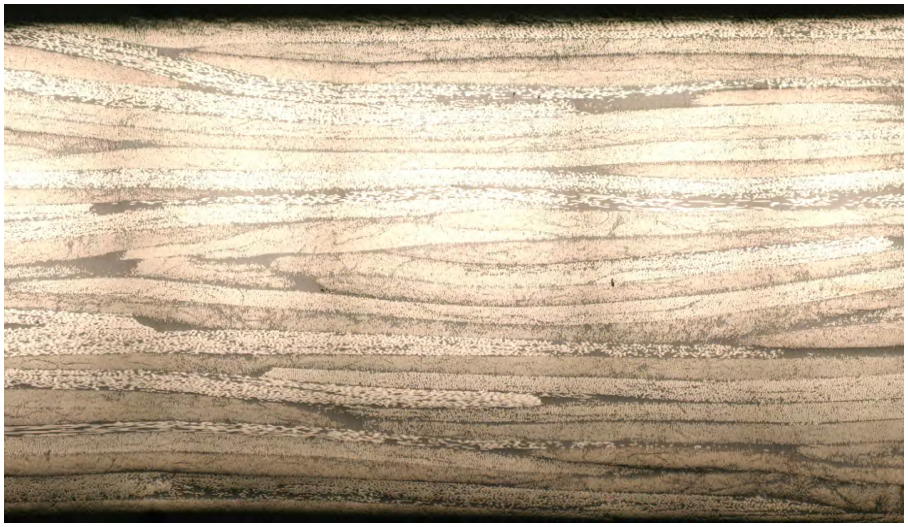

Figure 3. Micrographic section of polished specimen at 100x magnification.

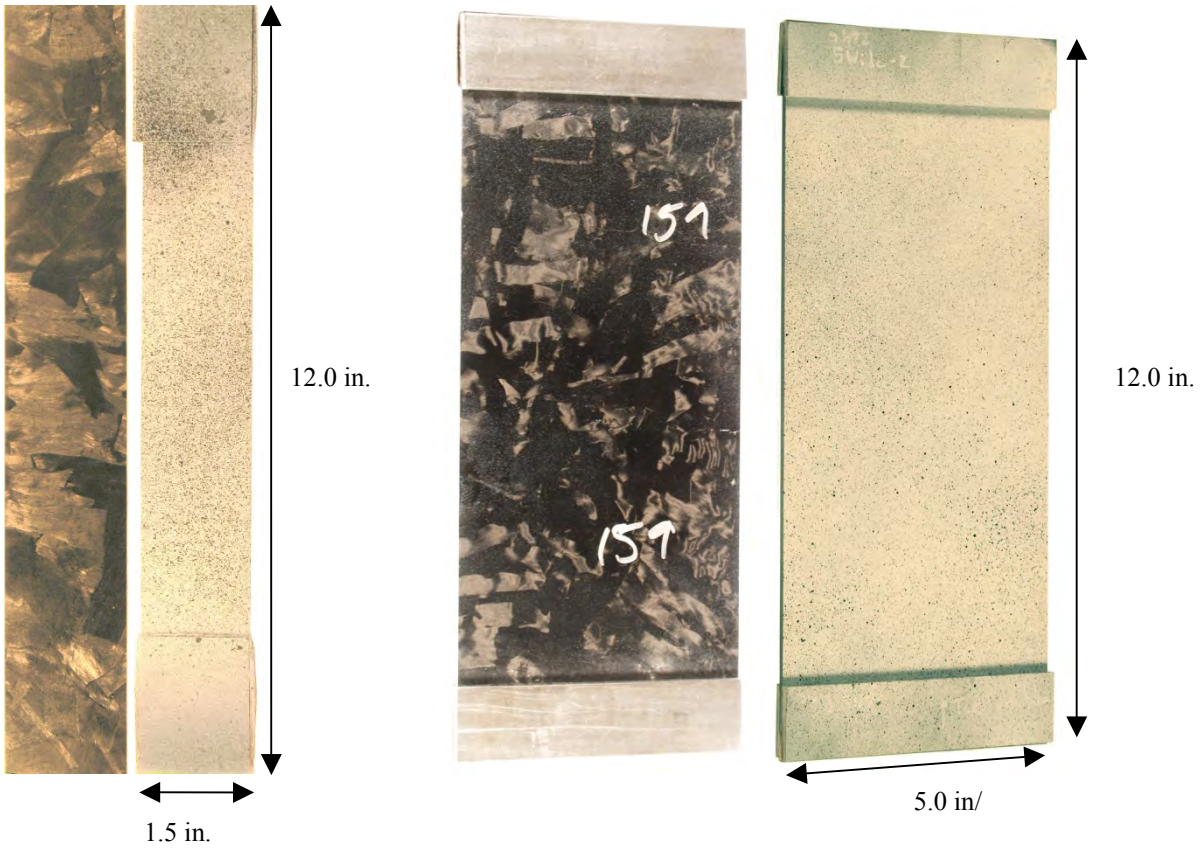

Figure 4. Two specimen geometries are used to measure full-field modulus via Digital Image Correlation, a small specimen (left) and a large specimen (right)

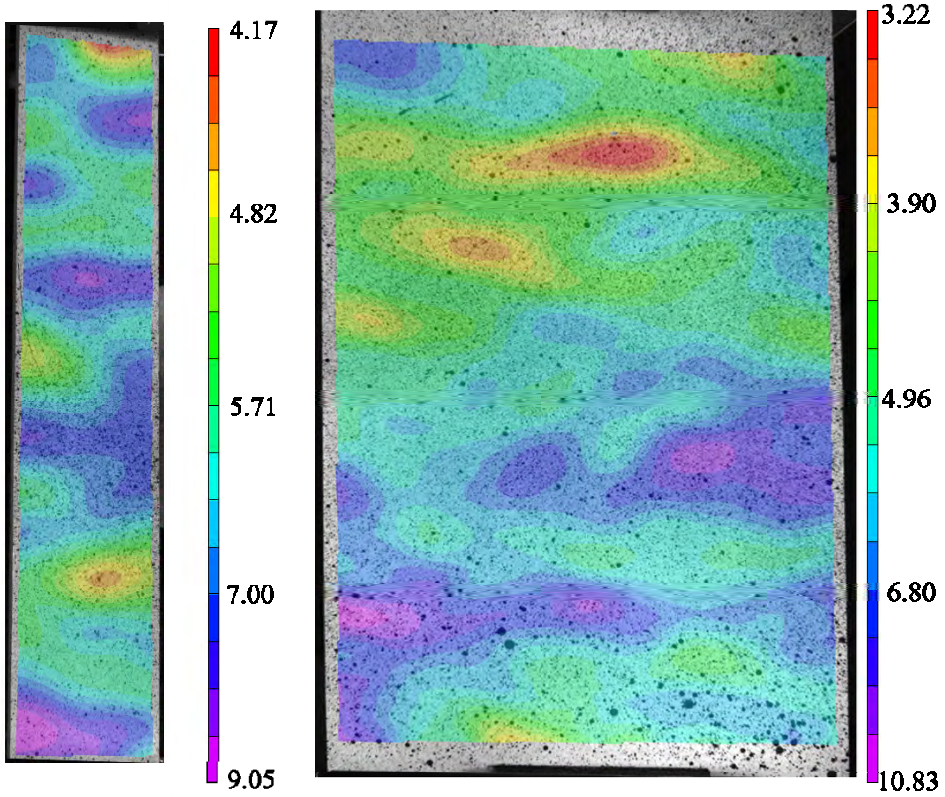

Figure 5. Example of DIC results for the small and the large specimen, with axial elastic modulus reported in Msi.

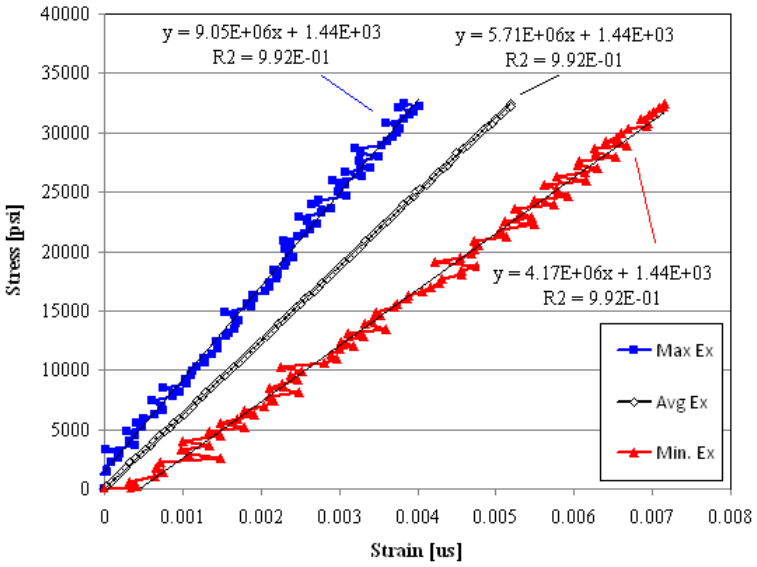

Figure 6. Stress-strain elastic curves corresponding to maximum, average and minimum moduli as measured via DIC on a single small tension specimen.

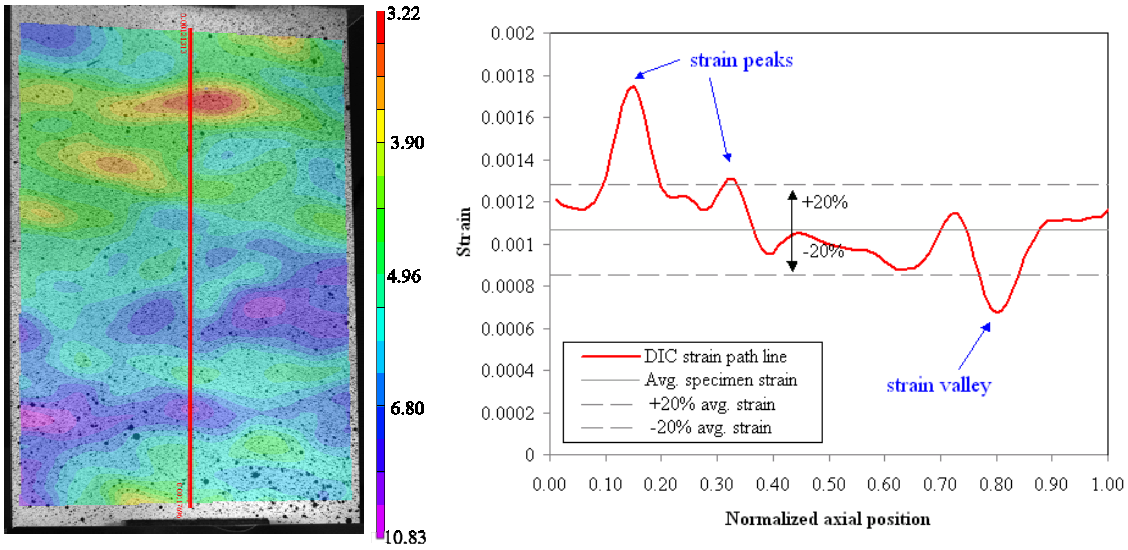

Figure 7. The variation of the axial strain along the path line can be plotted against the normalized location along the line. In the plot average full-field strain for the specimen is plotted together with ±20% upper and lower bounds.

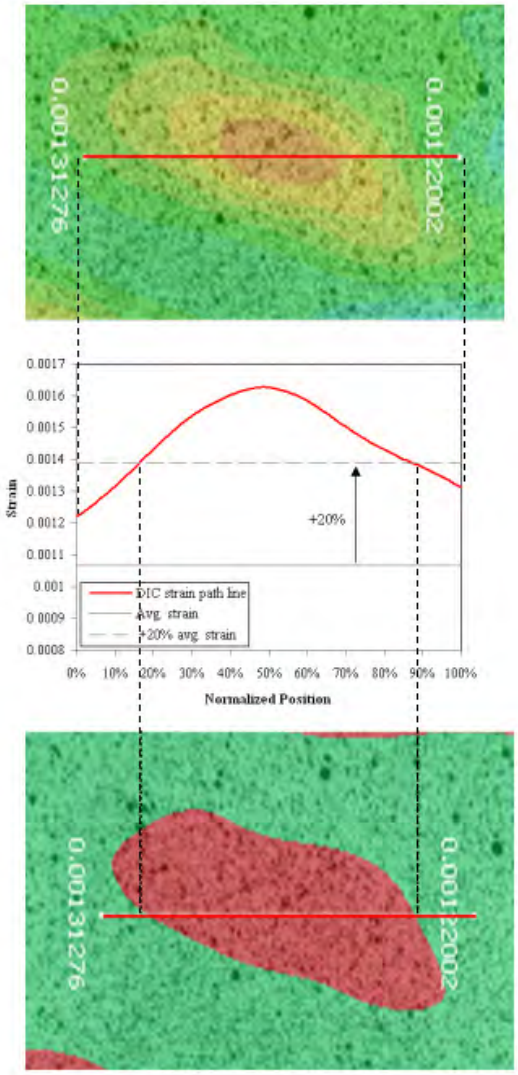

Figure 8. Example of application of the "filtering" scheme to isolate the region of strain exceeding the average specimen strain by at least +20%

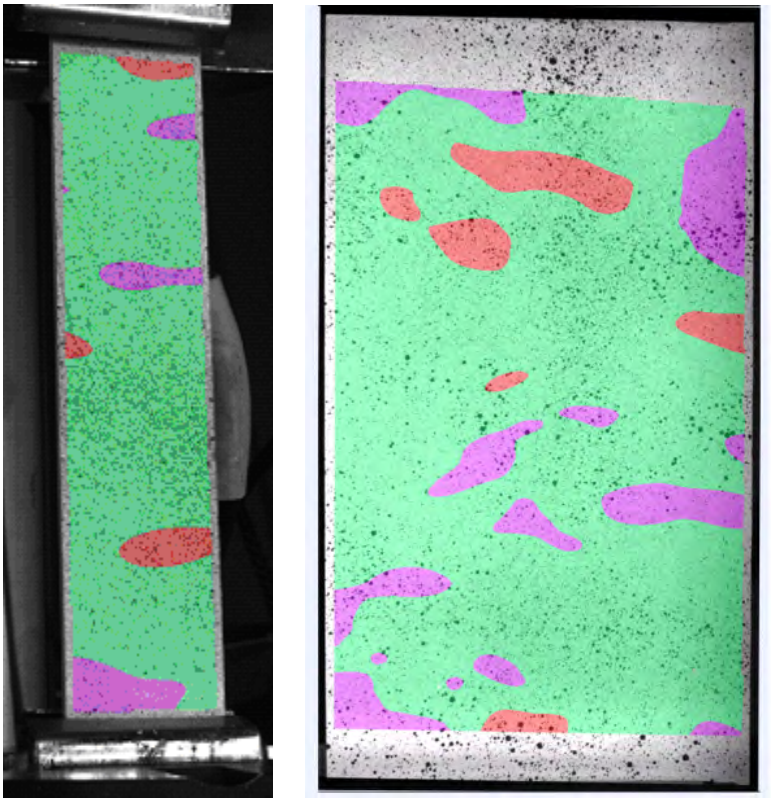

Figure 9. Application of the filtering scheme to the two specimens of Figure 5 enables the identification of areas that exceed the average specimen modulus by ±20%.

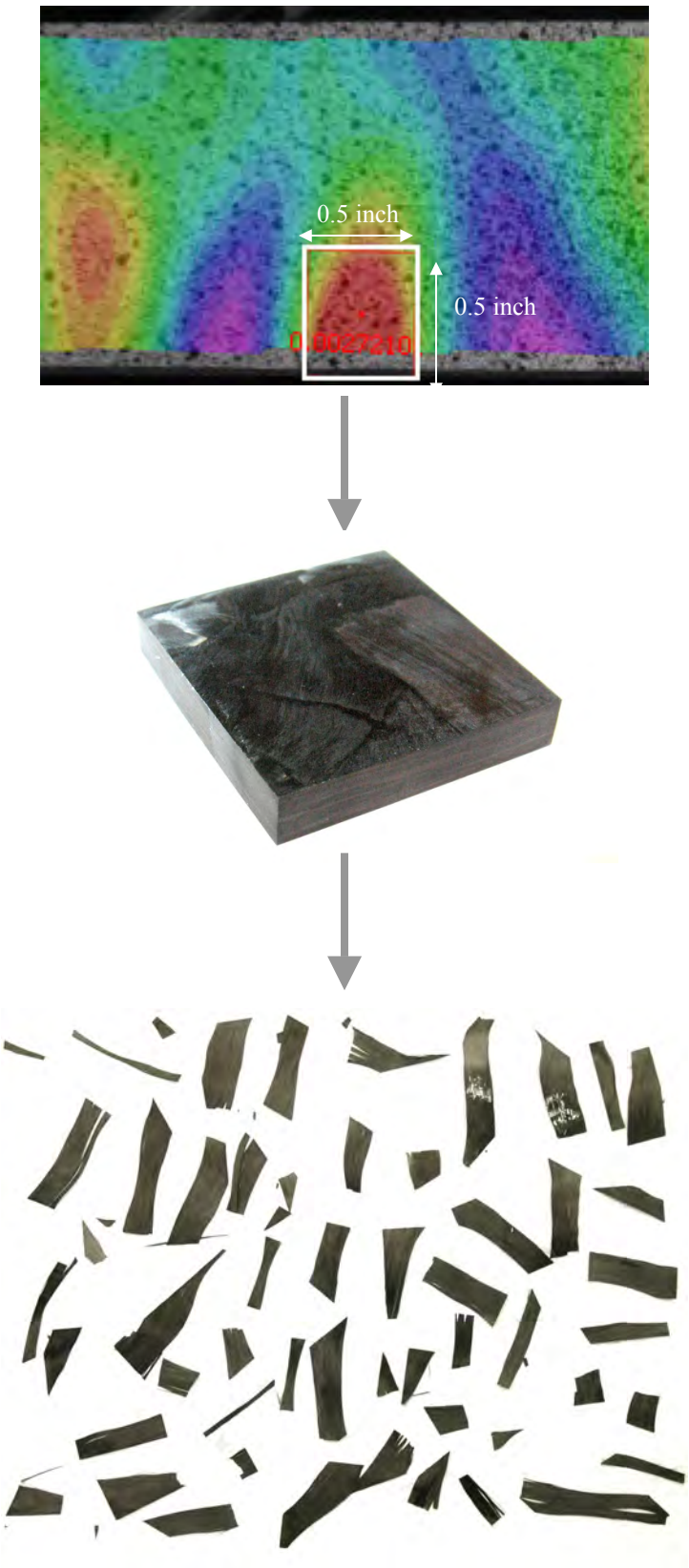

Figure 10. Based on the average size of approximately 0.250 in^2, a 0.5 in. square section of material is cut out for subsequent burn-off and deplying to separate the single chips and portions of chips.

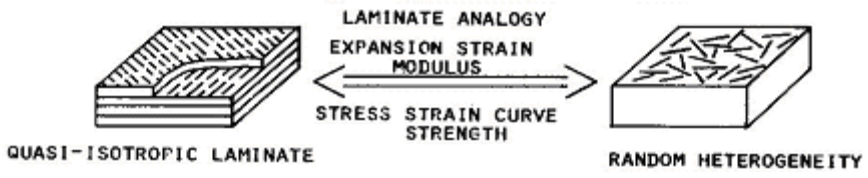

Figure 11. Original laminate analogy for discontinuous fibers as proposed by Halpin and Pagano [2]

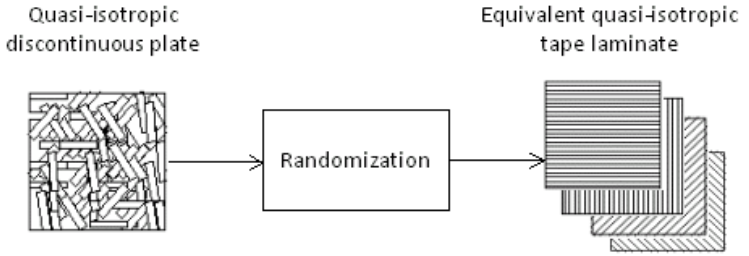

Figure 12. Schematic of the modified laminate analogy proposed in this study.

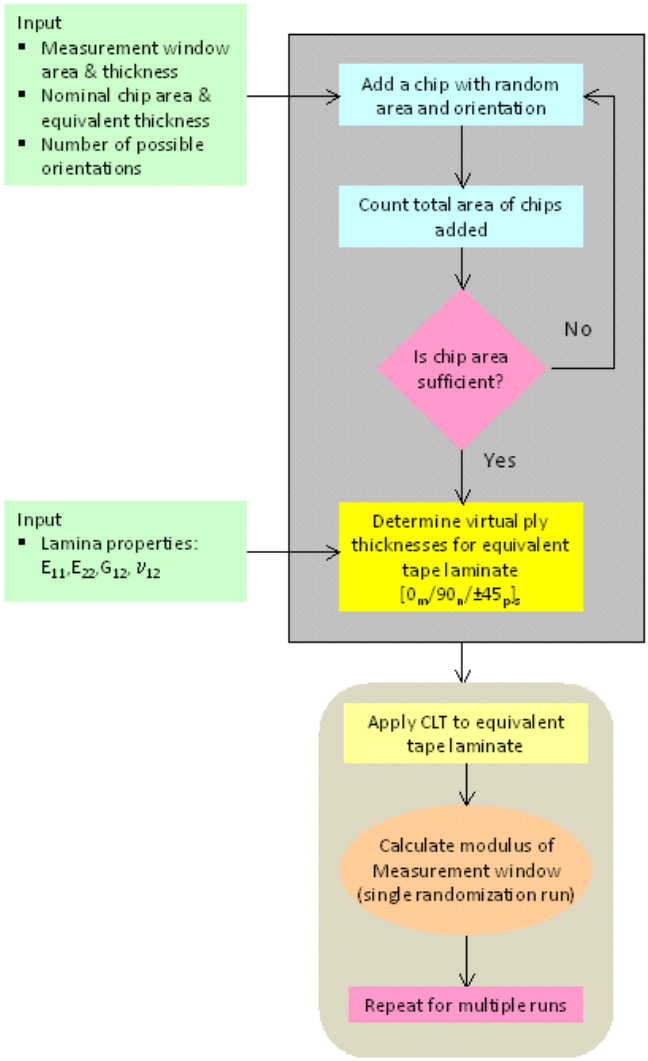

Figure 13. Flow chart indicating the logical process, inputs and outputs of the randomization and laminate analogy

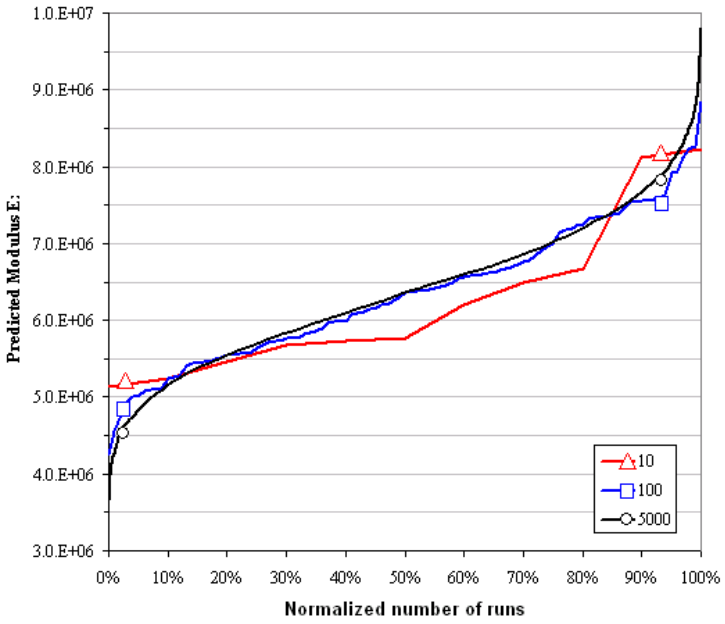

Figure 14. Predicted modulus distribution (from min. to max., left to right) for 10, 100 and 1,000 runs for a measurement window of an RRVE, resulting in a CoV of 14.8%.

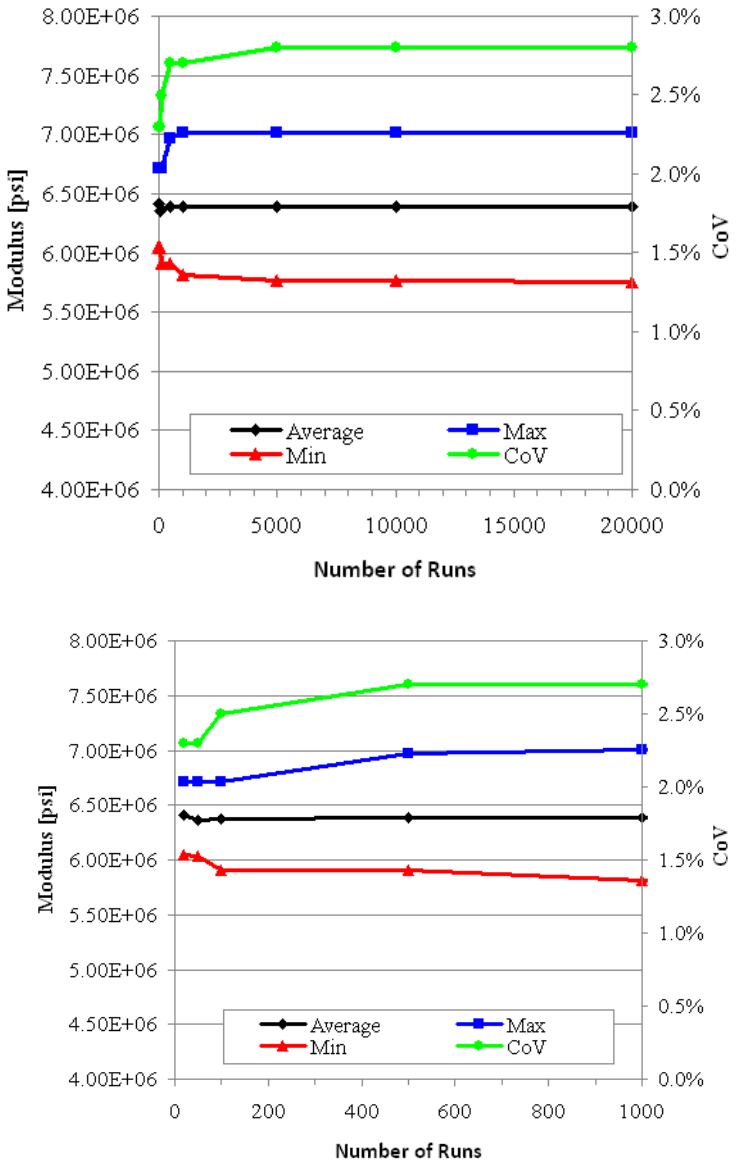

Figure 15. Convergence of analysis with number of runs shows asymptotic trends for average, max and min moduli up to 20,000 runs (top) and detail of the transient region for fewer runs (bottom)

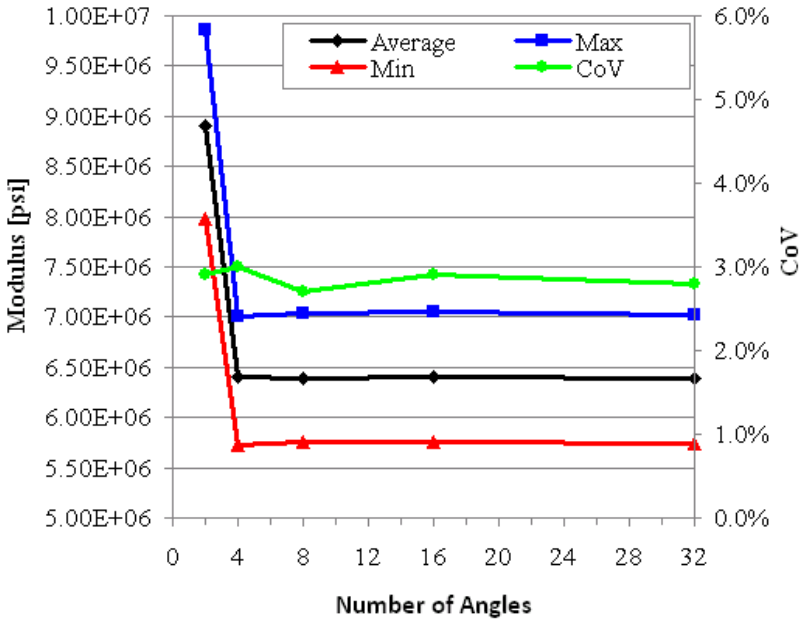

Figure 16. Modulus convergence with respect to allowed orientations for the random chips

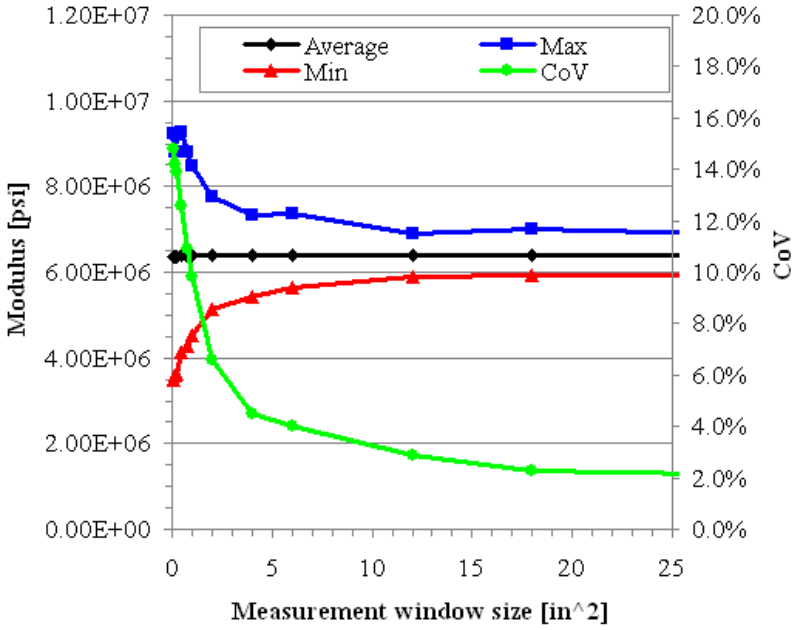

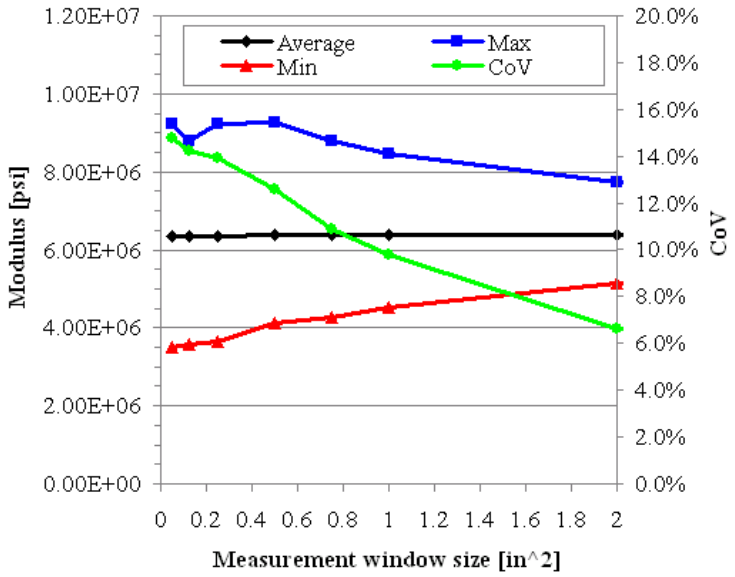

Figure 17. Maximum, minimum, average modulus and CoV variation with measurement window area

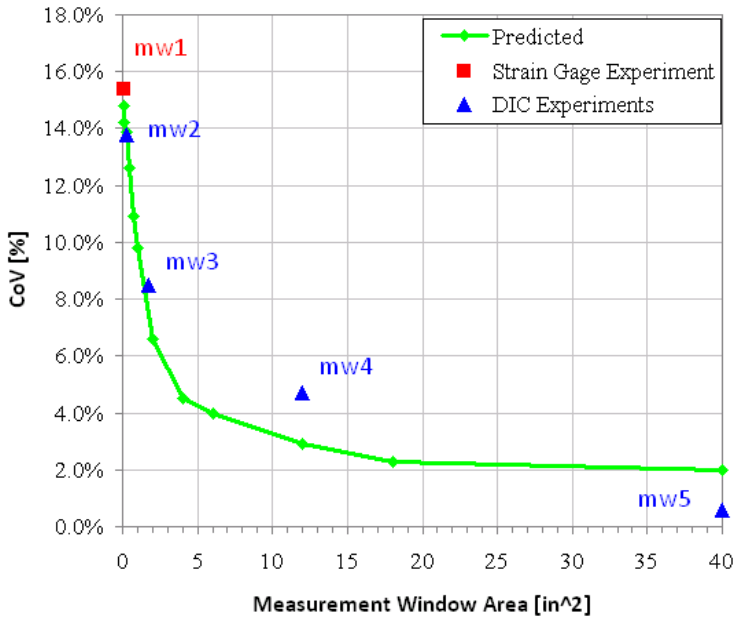

Figure 18. Comparison between predicted and experimental CoV results as function of measurement window area, as defined in TableV.

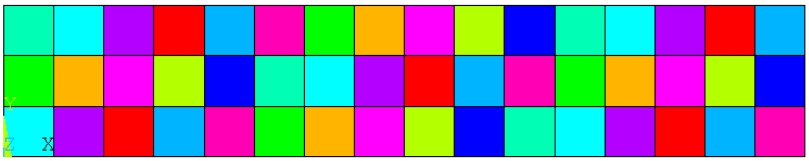

Figure 19. The small tensile specimen is divided into 48 regions, corresponding to the 0.25 in^2 (161 mm^2) RVE, with independently generated material properties.

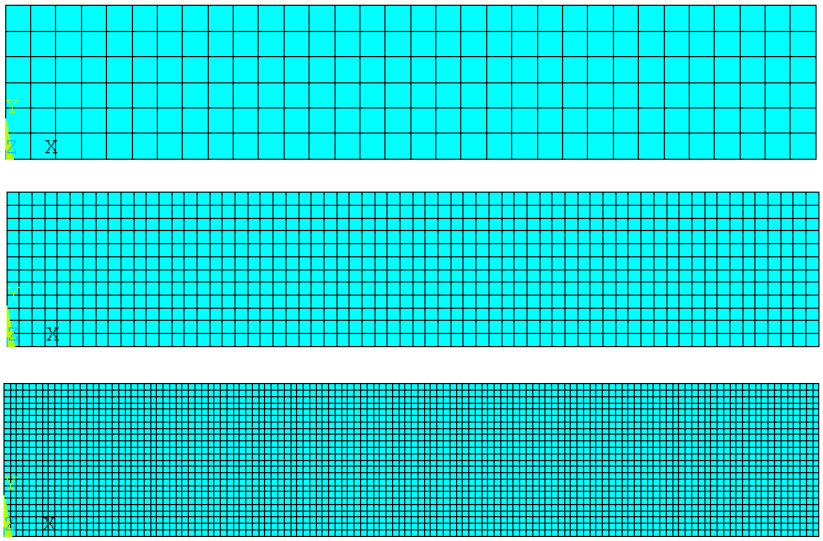

Figure 20. Three levels of mesh refinement (coarse, medium and fine from top to bottom) independent from the subdivision of the specimen into multiple RVE's.

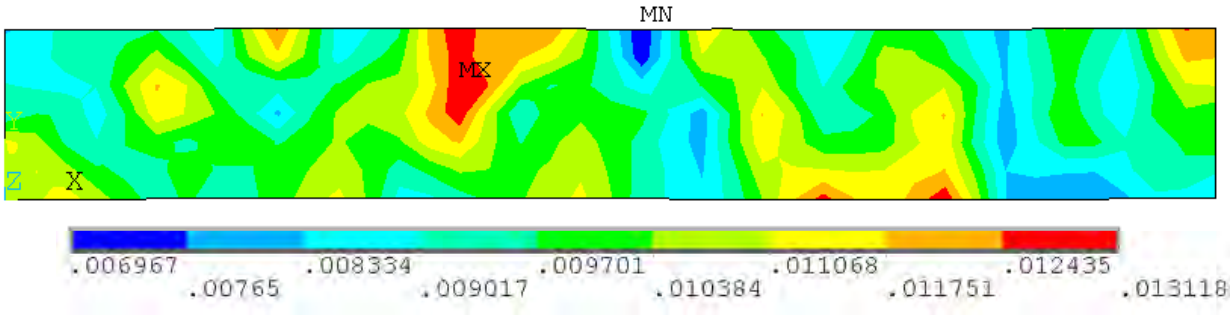

Figure 21. Typical results obtained from the FE model show areas of peaks and valleys in strain distribution along the specimen, similar to the experimental DIC plots of Figure 5, left.

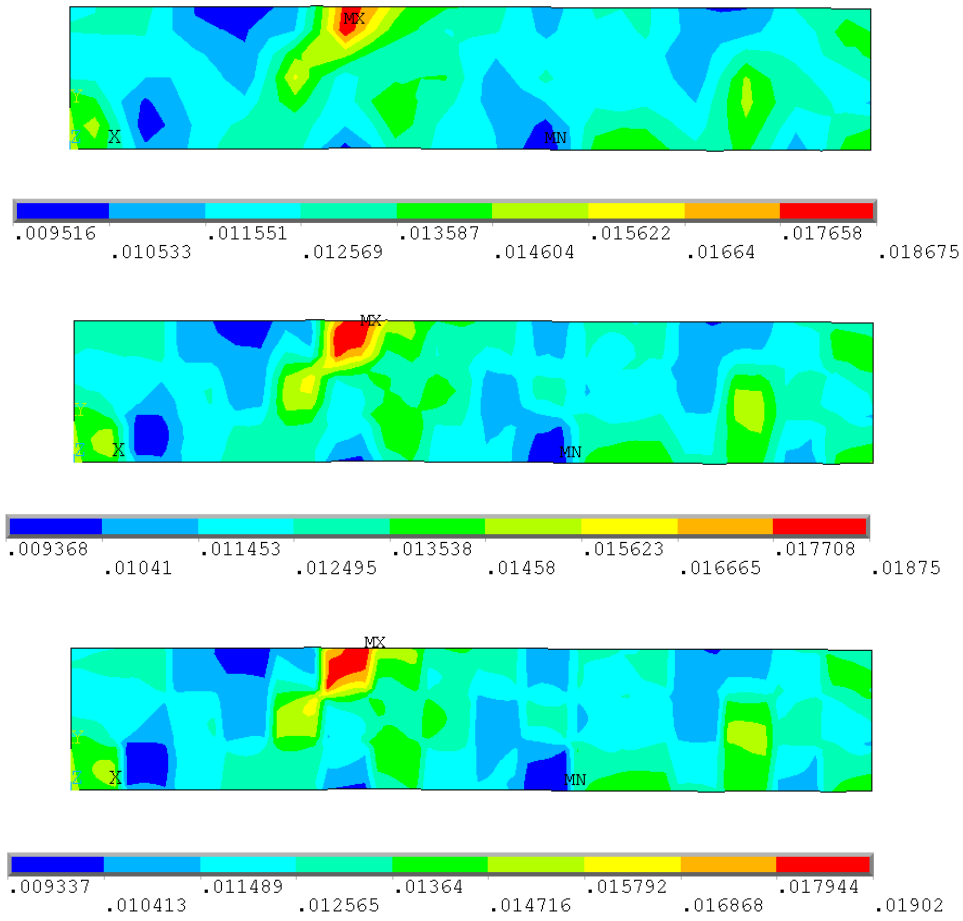

Figure 22. Another typical strain contour plot obtained from the FE model, showing little variation for increasing mesh size (coarse to fine, top to bottom).